Geophysical Research Letters

RESEARCH LETTER
10.1029/2019GL085730

Key Points:
- Submarine groundwater discharge (SGD) is prevalent in an area with thriving, biodiverse reefs
- SGD is associated with shallow-water hydrothermal vents that emit acidic waters and carbon dioxide
- The vents raise pCO_2 and lower pH over 1–2 km of coastline

Supporting Information:
- Supporting Information S1
- Movie S1
- Movie S2
- Movie S3
- Movie S4
- Table S1

Correspondence to:
M. B. Cardenas,
cardenas@jsg.utexas.edu

Citation:
Cardenas, M. B., Rodolfo, R. S., Lapus, M. R., Cabria, H. B., Fullon, J., Gojunco, G. R., et al. (2020). Submarine groundwater and vent discharge in a volcanic area associated with coastal acidification. *Geophysical Research Letters*, *47*, e2019GL085730. https://doi.org/10.1029/2019GL085730

Received 7 OCT 2019
Accepted 23 DEC 2019
Accepted article online 3 JAN 2020

Submarine Groundwater and Vent Discharge in a Volcanic Area Associated With Coastal Acidification

M. Bayani Cardenas[1], Raymond S. Rodolfo[2,3], Mark R. Lapus[2], Hillel B. Cabria[2], Jose Fullon[4], Gordos R. Gojunco[5], Daniel O. Breecker[1], Danica M. Cantarero[6], Jaivime Evaristo[7], Fernando P. Siringan[6], and Tongwei Zhang[8]

[1]Department of Geological Sciences, The University of Texas at Austin, Austin, TX, USA, [2]Agricultural Sustainability Initiatives for Nature, Inc., Quezon City, Philippines, [3]Department of Environmental Science, Ateneo de Manila University, Quezon City, Philippines, [4]Planet Dive Resort, Batangas, Philippines, [5]Scuba Academy Manila, Makati, Philippines, [6]Marine Science Institute, University of the Philippines-Diliman, Quezon City, Philippines, [7]Copernicus Institute of Sustainable Development, Utrecht University, Utrecht, The Netherlands, [8]Bureau of Economic Geology, The University of Texas at Austin, Austin, TX, USA

Abstract We investigated submarine groundwater discharge (SGD) in a volcanic coastal area that hosts the world's most biodiverse reefs. Measurements of ^{222}Rn activity in coastal seawater, a tracer for groundwater, indicated prevalent SGD. In areas where seawater ^{222}Rn activity was generally higher, we discovered hydrothermal springs emitting acidic waters (pH ~5.4–6.0) and venting magmatic CO_2 that brought local pCO_2 levels up to 95,000 ppm. The collection of vents raised CO_2 and lowered pH over 1–2 km of coastline. The hydrogen and oxygen isotope compositions of water and chloride concentration revealed that the springs discharge recirculated seawater mixed variably with terrestrial groundwater. Shallower springs and pore water have a higher proportion of terrestrial groundwater than deeper springs, which emit mostly recirculated seawater. This suggests that different SGD mechanisms are present. The SGD could be contributing to the evolution and function of the biodiverse ecosystem, but it also represents myriad pathways for contamination.

Plain Language Summary Groundwater flow from land to sea could have important coastal impacts but it is usually unrecognized. Delicate reefs may be particularly sensitive to groundwater inputs. Yet few studies have made connections between groundwater and reefs. We investigated submarine groundwater in a volcanic coastal area that hosts the world's most biodiverse reefs. By measuring ^{222}Rn activity in seawater as a tracer for groundwater, we found that groundwater discharge is prevalent throughout the coast. In areas where seawater ^{222}Rn activity was higher, we discovered hydrothermal springs emitting acidic waters (pH ~5.4–6.0) and venting volcanic CO_2 that brought local pCO_2 levels up to 95,000 ppm. The collection of vents raised CO_2 and lowered pH over 1–2 km of coastline. The composition of water samples indicates that the springs discharge recirculated seawater mixed variably with terrestrial groundwater. Shallower springs and pore water from the seabed have a higher proportion of terrestrial groundwater than deeper springs, which emit mostly recirculated seawater. These waters also interact more with the aquifer matrix. Because different mechanisms of groundwater flow from land to sea are taking place, the groundwater flow could be contributing to the evolution and functioning of the ecosystem. However, groundwater also represents potential pathways for contamination released from land.

1. Introduction and Background on the Site

Coastal ecosystems are critical to society (Barbier et al., 2011). Understanding their resilience and vulnerabilities in the face of climate change and human disturbance is necessary for their sustainable management (Hughes et al., 2003). They are vulnerable to degradation caused by land-derived inputs such as sediment and solutes delivered by rivers (Barbier et al., 2011). Submarine groundwater discharge (SGD) has been recognized as a pathway for solutes to enter coastal waters (Moore, 1996), suggesting an additional but unseen input and vulnerability originating from land (Sawyer et al., 2016).

Coral reefs are a critical feature of coasts that provide ecosystem services to hundreds of millions of people (Barbier et al., 2011; Spalding & Brown, 2015). In the Philippine marine biodiversity epicenter (Roberts et al., 2002) where this study was conducted, each square kilometer of reef provides $140K of economic value per year (Tamayo et al., 2018). Reefs are a threatened coastal resource with some potentially facing extinction (Carpenter et al., 2008). In addition to direct human disturbance, harm to reefs can come from the effects of increasing atmospheric CO_2 levels, which causes acidification. The negative effects of reef acidification have been studied by taking advantage of shallow-water vents that emit CO_2 (Fabricius et al., 2011; Goffredo et al., 2014; Inoue et al., 2013; Munday et al., 2014). Even in places with no CO_2 vents, acidification can be due to discharging acidic groundwater (Crook et al., 2013). These studies all show that hydrogeologic processes can have an impact on coral reefs. The recognized threats to coral reefs originating from land (Roberts et al., 2002) have excluded SGD however. This is a critical gap especially since it has been shown through global analysis of coastal watershed hydrologic budgets that SGD is pronounced, if not highest, in areas with thriving coral reefs, particularly along the active plate boundaries in Southeast Asia and the Coral Triangle (Zhou et al., 2019). In fact, historical increases in groundwater nutrient concentrations from agricultural development have been recorded in coral skeleton in degraded reefs (Erler et al., 2018). This problem may be more common than recognized.

We studied an area that is at the center of what has been referred to as the "center of the center of marine biodiversity" in the world (Carpenter & Springer, 2005)—the Verde Island Passage in the Philippines. The region's geology, tectonic setting, and hydroclimatology are representative of many parts of the Philippines and are similar to other islands in Southeast Asia. The study area—Calumpan Peninsula (Figure 1a and supporting information Figure S1)—separates Balayan Bay to its west from Batangas Bay to the east. The peninsula, which hosts the town of Mabini, has: Miocene to Pleistocene age, fractured and thus potentially highly permeable volcanic rocks (del Rosario & Oanes, 2010); numerous faults including its linear coastline that could serve as fluid pathways; high rainfall of 1,800–2,000 mm/year (Funk et al., 2014), which promotes high rates of groundwater recharge and downgradient discharge; relatively small watersheds that funnel water into ephemeral rivers; and high relief. The site is within the so-called Macolod Corridor volcanic rift center (Forster et al., 1990) that includes a major active volcano (Taal Volcano) and is geothermally active (del Rosario & Oanes, 2010). There are two major faults near the site—the Verde Island Passage Fault and its splay, the Lubang Fault. The favorable combination of factors above led us to postulate that SGD is significant throughout the peninsula and that it may have different drivers including volcanic-hydrothermal phenomena.

Mabini has many long-established marine protected areas along its coast. Recreation and tourism, particularly catering to scuba divers, have become the main driver of its economy and an alternative source of income for many locals who used to be fishers (Christie, 2005; Samaniego & Rebancos, 2019). The boom in tourism could harm the reefs if the terrestrial-marine connections are not adequately recognized, understood, and included in management and policy decisions. While nutrient-poor reefs may receive more of their needed nutrient inputs from groundwater than rivers (Kim et al., 2011), with contamination of aquifers near the coast, this could lead to damaging eutrophication of reefs that lasts over decades (Tait et al., 2014). The extent to which groundwater inputs and hydrogeologic processes are actively occurring and whether they are good or bad for the reefs and shores of the study site in the Philippines are largely unknown. We sought to determine the presence of coastal and SGD to identify the different forms or mechanisms of their occurrence and its impacts on coastal waters.

2. Methodology

This study was conducted over a period of 3 years (2016–2019). The field effort included exploration for submarine springs and on-land springs and wells, development of techniques, collection of samples, and in situ measurements. First we determined the presence of SGD (representing both fresh groundwater from land and saline groundwater recirculating through the coastal sediment and aquifer) by measuring ^{222}Rn activity in coastal seawater around the peninsula. Complementing this are ^{222}Rn activity measurements of discrete water samples from domestic wells and from springs on-land and offshore. Water from the same locations were also analyzed for major ion chemistry and isotopic composition ($^{2}H/^{1}H$, $^{18}O/^{16}O$, and $^{17}O/^{16}O$), and their pH and specific conductivity were measured on-site. Sources of the water samples analyzed were

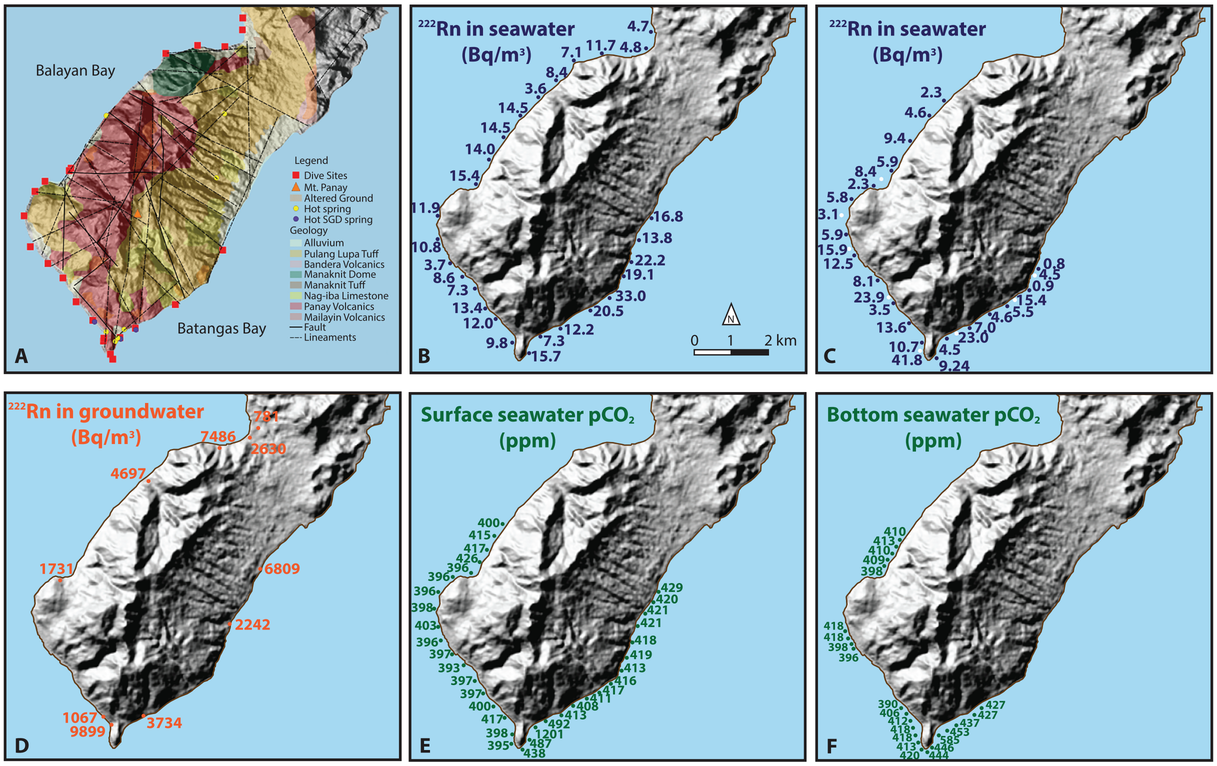

Figure 1. Key geologic features at the study site and results of ^{222}Rn and pCO$_2$ measurements. Panel a shows the main geologic formations in the area, which are mostly volcanic rocks. It also shows several faults and lineaments. Several popular dive sites are denoted by red squares. Panels b and c show results of underway ^{222}Rn measurements at different locations denoted by dots; the surveys were conducted in April 2016 (panel b), April 2017 (white dots in panel c), and July 2017 (blue dots in panel c). Panel d shows measured ^{222}Rn concentrations in groundwater taken from on-land wells. Panels e and f show measured in situ pCO$_2$; the results in panel e are from underway measurements of seawater conducted from a boat, and the results in panel f are from in situ bottom-water measurements conducted while scuba diving along the 15-m isobathymetric line.

determined by visualizing along a binary mixing line. Finally, upon discovering shallow hydrothermal vents at a few locations, we also measured in situ pH and pCO$_2$ of surface and bottom seawater with a submersible infrared CO$_2$ analyzer. Underwater in situ measurements were done through scuba diving along the seabed at a fixed depth or at specific sites, that is, right at the springs and vents. The vents included bubbles of gas seeping from the seafloor. Gas samples were thus collected in situ by scuba divers and then analyzed for their chemical and carbon isotopic (^{13}C/^{12}C) composition. The underwater measurements and exploration are presented in Movies S1–S4. The suite of approaches allowed for simultaneous characterization of SGD across the region and right at and near the points of discrete discharge. It led to a conceptual picture for SGD and the hydrogeology of the site. Further details on the methods are provided in the supporting information.

3. Groundwater Tracing Reveals the Prevalence of Discharge Along the Coast With Some Hot Spots

We found that coastal seawater has a persistent signal of groundwater, with ^{222}Rn activities ranging from 0.8 to 41.8 Bq/m^3 with an average of 11.1 Bq/m^3 (Figures 1b and 1c). Open seawater had no measurable ^{222}Rn. Groundwater samples from domestic wells in the peninsula have expectedly high ^{222}Rn activity, from 781 to 9,899 Bq/m^3 with an average of 4,107 Bq/m^3 (Figure 1d), and water from two submarine springs have even higher concentrations (7,092 and 14,947 Bq/m^3; Table S1). The seawater ^{222}Rn signals were present during the different times we conducted synoptic measurements. ^{222}Rn hotspots (strong signals) are always present along the coast (Figures 1b and c), with higher activities generally found in the southeastern coast of the peninsula. We found shallow-water hydrothermal vents (SHVs) releasing thermal waters through discrete submarine springs and gases through bubble plumes (Figure 2) at the southeastern coast.

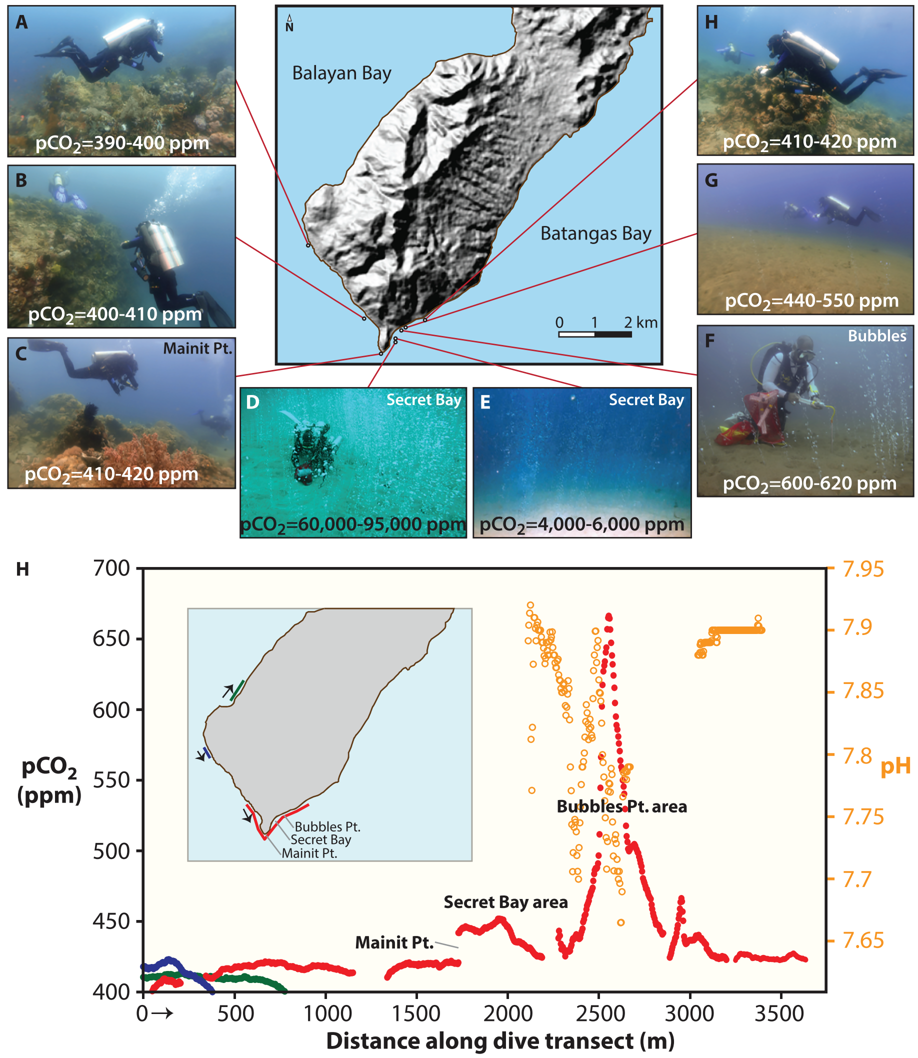

Figure 2. Panels a–i shows results from some in situ pCO_2 measurement transects throughout Mabini, Batangas, Philippines. The map shows the location of the sites, denoted by dots. The sites are connected by the red lines to their corresponding pictures that show the pCO_2 (ppm) ranges. Panel h shows results of continuous, in situ pCO_2 measurements and some in situ pH measurements from dive traverses along the 15-m isobathymetric line. The two main areas with dramatic shallow hydrothermal vents are in Secret Bay and Bubbles Point. The points in Figure 1f are a subset of the points presented in panel h. Most of the thriving reefs are found in the west (a–c) where pCO_2 is more typical, whereas the seabed tends to be comprised of sediment and patchy reefs in the east (d–h) where the springs and CO_2 vents are present. The pictures in a, b, c, g, and h show a diver with the in situ, real-time CO_2 sensor.

4. Carbon Dioxide Vents and Acidification of Coastal Waters

The SHVs in the southeastern coast were typically identified by dramatic gas vents or sometimes by the presence of pockmarks and repeating conical mounds (Figure 2). Bubbles were usually seen first and then thermal springs were often found upon closer inspection. Samples of gas from the vents were found to be composed of more than 90% CO_2. The $\delta^{13}C$ values of these samples ranged from −6.8 to −7.3‰ (see Table S1). Biogenic CO_2 can be ruled out as a source since these are isotopically much lighter ($\delta^{13}C$ of −23‰ following Sharp, 2006). Our measured $\delta^{13}C$ is consistent with observed and theoretical $\delta^{13}C$ values for CO_2 degassed from magma in Kilauea Volcano, which varied from −7.8 to −3.4‰ (Gerlach & Taylor, 1990). The average for reported CO_2 $\delta^{13}C$ of approximately −4‰ (Chiodini et al., 2008) from the Solfatara in Pozzouli Volcano is also near our values. Thus, the CO_2 at the site is most likely of magmatic origin and ultimately sourced from mantle materials, both of which have $\delta^{13}C$ of approximately −6‰ (Sharp, 2006).

Since the CO_2 vents and groundwater discharge are connected, we later surveyed the concentration of CO_2 (or partial pressure pCO_2) in surface seawater through underway measurements with an infrared CO_2 analyzer. Additionally, the pCO_2 of bottom water at a depth of 15 m was measured in situ using the same instrument operated in autonomous mode. The latter measurements are referred to as "bottom water" to distinguish them from surface seawater. Hotspots of seawater pCO_2 were found in roughly the same locations as the ^{222}Rn hotspots in the southeastern part of the peninsula (Figure 1e). Seawater pCO_2 reached as high as 1,200 ppm near a ^{222}Rn hotspot area (Figures 1c and 1e). From the southern tip of Calumpan Peninsula, which is called Mainit Point, seawater pCO_2 remained at around and over 430 ppm over roughly a kilometer-long section of the coast going to the east (Figure 1E). The bottom-water pCO_2 was similarly high over the same area (Figure 1F). In the west and north of Mainit Point, seawater and bottom-water pCO_2 were always lower compared to the east of it.

We identified two major areas where gas vents are concentrated. One area is at the locale called Secret Bay that is immediately east of Mainit Point. Another is a dive site further to the east referred to fittingly as Bubbles Point or "Bubbles" for short (Figure 2h). The bottom-water dive transects (shown in Figures 1f and 2h) did not purposely overlap with any SHVs; divers carrying the CO_2 sensor swam at a constant pace along the planned depth following the seabed while ignoring the presence or absence of seeps and SHVs. The bottom-water transect therefore measured the ambient pCO_2 levels in the area. There is a clear increase in bottom-water pCO_2 transitioning from west to east of Mainit Point, from about 420 to 450 ppm (Figure 2h). The bottom-water pCO_2 remained above 420 ppm across the Secret Bay area. Further eastwards, across the Bubbles Point area, the bottom-water pCO_2 ranged from approximately 450 to 675 ppm. The increase in pCO_2 in Bubbles was accompanied by a drop in in situ measured pH of 0.25 units, from 7.91 to 7.66 (Figure 2h). pH was measured separately by a submersible sensor with a pH electrode.

Taking the CO_2 sensor to the discharge points revealed what are likely the highest local pCO_2 values measured in coastal waters. The most dramatic levels were found in an area with relatively deep bubble vents. This area, hereafter named Soda Springs, is at a water depth of 55 m and is within Secret Bay (Figure 2d and Movies S1 and S2). pCO_2 ranged from 60,000 to 95,000 ppm right at Soda Springs. A few tens of meters away from Soda Springs and toward the shore is a broad sandy area at a depth of 50 m with curtains of bubble streamers (Figure 2e and Movies S1 and S2). The pCO_2 at this site ranged from 4,000 to 6,000 ppm (Figure 2e). The pH of a water sample collected at this site was 6.65. Closer to the coast, about 100 m going toward land from Soda Springs, the pCO_2 of bottom water at 15-m depth across Secret Bay ranged from 420 to 450 ppm (Figure 2h). At the surface in Secret Bay, no bubbles are visibly obvious, and most of the gas bubbles have redissolved before reaching the surface. The pCO_2 in an area with SHVs and lots of bubble streamers in Bubbles Point, which gives the site its name, ranged between 600 and 620 ppm (Figure 2f). On the western side of the peninsula, the pCO_2 of both surface seawater and bottom seawater are more typical of nonacidified seawater, with levels staying below 420 ppm (Figures 1 and 2).

5. Acidic Thermal Springs and Subsurface Mixing of Discharged Groundwaters

The SHV springs emit acidic thermal waters with a measured pH range of 5.42–6.85 (Table S1), which is much lower compared to open seawater with a pH of 8.11 measured hundreds of meters offshore. In situ temperatures measured with conductivity–temperature–depth probes range from 50 °C to 55 °C at the point of discharge. Discrete samples of the coastal seawater within a few tens of meters off the coast and where SHVs are present have a pH of 6.50–7.90. The samples from the submarine springs are all $Na\text{-}Cl\text{-}SO_4$ waters (like seawater) and have a specific conductivity very close to seawater (Table S1).

The source of SHV spring waters was determined through visualization along a binary mixing line using what is postulated as a pure groundwater sample as one end-member and open water seawater as the other. The groundwater end-member is a sample taken from a shallow open domestic well. This water was the freshest sample we encountered (see sample GW in Table S1 and well location in Figure S2). Its isotopic composition also shows that it is recharged precipitation. GW falls directly on the global meteoric water line (Figure 3a), and its deuterium excess ($d = \delta^2H\text{-}8\cdot\delta^{18}O$; Figure 3d) of 10.28‰ is similar to precipitation; from Global Network of Isotopes in Precipitation stations, the d for rainfall in the Philippines is 12.8 ± 2.3‰ (the Manila station nearest to our site has $d = 8.8‰$). δ^2H, $\delta^{18}O$, and chloride were considered in the mixing line

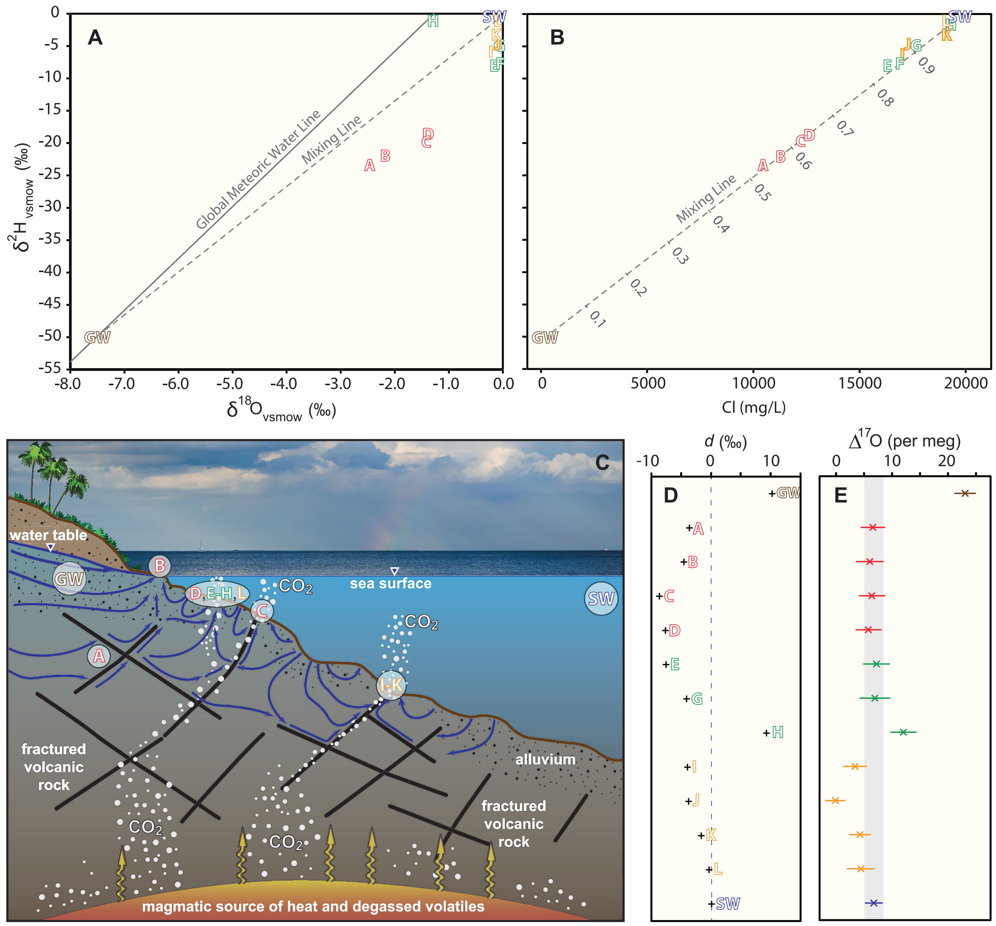

Figure 3. Panels a, b, d, and e show the isotopic and chloride composition of water samples; panel d shows the deuterium excess (*d*), and panel e shows the ^{17}O excess ($\Delta^{17}O$). The horizontal bars in panel e denote the analytical error. The letter labels denote the following: GW, terrestrial groundwater; a to d, on-land and shallow submarine springs; e to h, pore water from seabed sand; and i to l, relatively deep submarine springs. Panel c shows a conceptual interpretation of the hydrogeology of the study area based on locations of water samples and their seawater proportions (i.e., the decimal values along the mixing line in panel b). Note that the diagram is conceptual and not necessarily to scale. Table S1 provides further details on the sample location and chemistry. The locations where the samples are from and pictures of the sites are found in the supporting information figures.

calculation; the proportion of groundwater versus seawater is readily apparent based on visual inspection of a sample's location along this line. The samples fell to the right of the mixing line in δ^2H-$\delta^{18}O$ mixing space (Figure 3a). This shift might either be due to evaporation or geothermal fluid-rock interactions (Sharp, 2006) or mixing with magmatic waters (Yardley, 2009). However, all samples fell closely along the conservative mixing line in δ^2H-Cl space (Figure 3b). This suggests that some samples have experienced an ^{18}O shift, which might be explained by geothermal processes (Sharp, 2006).

The location of the samples along a binary mixing line revealed that the SHV spring waters are mostly of seawater composition (50% or more) but with some mix of terrestrial groundwater. The water samples show a clear progression of mixing (Figure 3; see Table S1 for complete description, and see Figure S2 for sampling locations). A sample discharging from a groundwater well close to the coast whose water is used to fill a hot spring pool at Sea's Spring Resort (sample A) and a sample from a hot spring located at the beach in front of Planet Dive Resort, which gets exposed during very low tides (sample B; see Figure S3 for a picture of the site), have the highest proportions of mixed-in groundwater. These are then followed by samples from submarine springs that are relatively shallow (6–9 m of water depth; samples C and D; see Figure 3 for pictures). Pore water samples (samples E–H; see Figure S5 for pictures) showed a clear progression of having more groundwater mixed-in with increasing depth within the sandy seabed. This progression was accompanied by decreasing specific conductivity (Table S1). Water from deeper submarine springs had seawater fraction of upwards of 85%. Deeper springs at Bubbles (samples J and K in figures and tables; see Figure S6 for pictures) were discharging water that was more than 90% seawater. However, water discharging from a very deep spring at Soda Springs (sample I; see Figure 2d) had relatively and slightly more groundwater mixed-in with it, with 88–90% seawater fraction.

The clustering of water samples is also apparent in their isotopic composition (Figure 3). The *d* of samples A to D, whose order also follows increasing seawater fraction, progressively became more different from GW, and the *d* of samples I–L progressively became more similar with SW. Samples A–D, which have higher fractions of terrestrial groundwater also exhibit strong ^{18}O shifts relative to the conservative mixing line (Figure 3a), indicating more extensive geothermal water-rock interactions. With the exception of sample H, samples E–L have δ^{18}O similar to SW, indicating little to no water-rock interactions. A positive shift in ^{18}O results in smaller (more negative) *d*. The expected pattern in *d* associated with a positive ^{18}O shift is seen in Figure 3d—samples A–D have the smallest *d*, whereas samples I–L have *d* values that become progressively similar to SW. Sample H is unique among all samples in that it is similar to both GW and SW. In terms of δ^2H and Cl, it is like seawater but in its *d* and ^{17}O excess (or Δ^{17}O, see Figure 3e and supporting information), it is closest to GW. The ^{17}O excess of the samples, except for GW and H, which have high Δ^{17}O that are more similar to precipitation (Luz & Barkan, 2010), are close to that of SW (Figure 3e).

The submarine spring waters also contribute dissolved CO_2 to the coast. Spring waters were analyzed for pCO_2 using the same sensor that was used for the in situ measurements. The submarine spring waters from Bubbles, the source of samples J and K in Figure 3, had a pCO_2 of 29,550 and 38,364 ppm, respectively. Pore water samples collected from the seabed at Bubbles had even higher pCO_2 levels of 76,876 and 78,679 ppm. Water from a beach spring (sample B) and water from a deep domestic well at the Planet Dive Resort had a pCO_2 of 8,767 and 8,842 ppm, respectively.

6. Comparison With Other Similar Areas With CO_2 Seeps and Vents

Other studies of reefs with CO_2 seeps have also reported high pCO_2. In Milne Bay in Papua New Guinea, pCO_2 approached ~1,000 ppm (Fabricius et al., 2011). Higher values reaching 1,465 ppm were found off Iwotorishima Island, Japan (Inoue et al., 2013). Values as high as 52,000 ppm were found for some seawater samples near Ischia Island in Italy (Hall-Spencer et al., 2008). There, the investigators also reported that gastropod shell dissolution took place at such high pCO_2 levels. The highest pCO_2 we measured at Soda Springs is almost double that of the highest reported in Hall-Spencer et al. (2008). The rest of the coast of Calumpan Peninsula just east of Mainit Point, which has a pCO_2 range between 400 and 600 ppm, is ideal for investigating a reef whose CO_2 levels are what are expected for the next century (Hughes et al., 2017). Previous studies on coastal CO_2 vents did not simultaneously analyze groundwater discharge and thus did not explicitly make a connection between terrestrial and submarine hydrogeologic processes and flow paths. An exception is a study on the natural acidification around the submarine springs in Puerto Morelos, Mexico, which discharge acidic groundwater (pH of 6.70–7.30) (Crook et al., 2013). Very near (few meters) these springs where reduced coral calcification was observed, the pH was monitored to range from 7.15 to 8.05. In comparison, at the eastern side of Calumpan Peninsula where we observed springs, vents and higher ^{222}Rn activities, the pH ranged from 7.65 to 7.9 over about a kilometer of coastline. Model calculations have shown that the pH of the ocean can drop by 0.77 by the year 2300 (Caldeira & Wickett, 2003)—this would lead to the pH values we observed near the springs.

7. Conceptual Picture for SGD at the Site and its Implications

Different local and regional SGD mechanisms have been shown in different parts of the Philippines. As typical in other places, SGD can be driven by seaward water table gradients present in coastal unconfined aquifers comprised of unconsolidated alluvium (Cardenas et al., 2015), resulting in discharge across the intertidal to shallow subtidal zone. However, terrestrial SGD may extend offshore through faults and fractures (Cantarero et al., 2019) and exit through discrete openings that are either directly open to the sea or buried under sediment (Zamora et al., 2017). In addition to these mechanisms, SGD may be due to recirculation of seawater through sediment driven by wave and tidal pumping and through density-driven convection

(Santos et al., 2012). In volcanically active areas where pronounced geothermal gradients are present, thermal convection of groundwater near coasts and just beneath the sediment-water interface can be dramatic and lead to springs with high flow rates as found in the crater lake of Taal Volcano near the study site (Cardenas et al., 2012). We surmise that all the groundwater flow mechanisms described above are taking place around Calumpan Peninsula.

The results are synthesized into the conceptual interpretation depicted in Figure 3h that illustrates the SGD mechanisms and points to the specific water samples and their relative locations where the mechanisms manifest. Even if some of the SGD occurs through discrete features, mixing calculations show that some submarine spring waters could have as much as 45% terrestrial groundwater. This implies that although there is substantial outflow of land-derived groundwater, before being discharged into the ocean, these mix with seawater. These waters also interact extensively with the aquifer matrix. Pore waters extracted from 0.3 to 1 m within the sandy seabed under a few meters of seawater are compositionally up to 15% terrestrial groundwater. This high rate of mixing with seawater can be the result of density-driven flow due to salinity. That is, as focused terrestrial SGD flows through coastal sediment, it entrains some relatively dense seawater that has infiltrated the sediment. Moreover, the mixing can be driven by thermal convection within the sediment. SGD discharging along beaches and the subtidal zone is also easily mixed with seawater because of tidal and wave pumping.

The general increase in seawater proportion of the discharged spring waters with increasing depths indicates that groundwater flow mechanisms are different between springs near and at the beach and those that are deeper (>10 m). The deeper hot springs also have dramatic flow rates and are clearly coming out from discrete openings rather than exfiltrating from porous and permeable sediment. If the subsurface plumbing of the deep springs was perfectly connected to the aquifer on land, they should have relatively high proportions of groundwater given the high discharge rates. This was not the case; the dramatic deep springs were compositionally very similar to seawater. Given these observations, these deep springs are thus interpreted to be forced by thermal convection whereby seawater infiltration and exfiltration define convective flow paths that are then focused by discrete features such as fractures. The lower extent of water-rock interaction, indicated by smaller shifts in δ^{18}O and *d* closer to seawater, suggests that these flow paths are over short distances, have high flow velocities, or both.

The volcanic degassing of CO_2 in the region is driving the release of CO_2 bubbles. However, at depth within the aquifer, degassed volatiles from deep-seated sources should also be dissolving in groundwater. This would explain why all discrete groundwater samples analyzed for pCO_2 exhibited very high levels. Independent of free-phase CO_2 venting, groundwater is a source of CO_2 and acidity.

The multiple previously unrecognized SGD pathways in the area are likely important for its ecology. These pathways also represent an important vulnerability present throughout the peninsula. Development of Calumpan Peninsula is concentrated along the coastal highway, which enabled the proliferation of resorts. Mabini has no central sewage collection and treatment. Hence all infrastructures rely on septic tanks. Because the aquifers of the area are comprised of permeable, fractured volcanic rocks, any introduced fluids and solutes may reach the coast over short time scales. Given the prevalence of SGD at the site and its multifaceted nature, it is important that SGD be considered in the assessment, protection, and management of its coastal ecosystems, as well as in other similar sites in the Philippines and throughout Southeast Asia and the Coral Triangle.

Acknowledgments
The authors thank the staff of Planet Dive Resort and the local government of Mabini, Batangas, for their assistance. We thank Jayson Balaibo, Allen Mendez, and Arlene Tengonciang for the assistance with scuba diving. Mark Barry and Cyndel Kelly of Pro-Oceanus provided valuable technical support on the use of the Pro-CV CO_2 sensor; Pro-Oceanus also provided in-kind support. We thank Elco Luijendijk, an anonymous reviewer, and the editor for comments that helped improved the manuscript. This research was supported by the Geology Foundation at The University of Texas at Austin. MC, RR, ML, and FS conceptualized the study. MC, RR, ML, HC, JF, GG, and DC conducted fieldwork and collected samples. RR, DB, JE, and TZ conducted laboratory analyses: DB conducted the carbon isotope measurements; JE had the water isotopes analyzed; and TZ analyzed the gas composition. FS provided field equipment. MC and RR analyzed and synthesized the results. All data are available in the main text or the supporting information. The data are archived at and can be downloaded from https://doi.org/10.6084/m9.figshare.11414028.

References

Barbier, E. B., Hacker, S. D., Kennedy, C., Koch, E. W., Stier, A. C., & Silliman, B. R. (2011). The value of estuarine and coastal ecosystem services. *Ecological Monographs*, *81*(2), 169–193. https://doi.org/10.1890/10-1510.1

Caldeira, K., & Wickett, M. E. (2003). Anthropogenic carbon and ocean pH. *Nature*, *425*(6956), 365–365. https://doi.org/10.1038/425365a

Cantarero, D. L. M., Blanco, A., Cardenas, M. B., Nadaoka, K., & Siringan, F. P. (2019). Offshore submarine groundwater discharge at a coral reef front controlled by faults. *Geochemistry Geophysics Geosystems*, *20*(7), 3170–3185. https://doi.org/10.1029/2019gc008310

Cardenas, M. B., Bennett, P. C., Zamora, P. B., Befus, K. M., Rodolfo, R. S., Cabria, H. B., & Lapus, M. R. (2015). Devastation of aquifers from tsunami-like storm surge by Supertyphoon Haiyan. *Geophysical Research Letters*, *42*(8), 2844–2851. https://doi.org/10.1002/2015gl063418

Cardenas, M. B., Lagmay, A. M. F., Andrews, B. J., Rodolfo, R. S., Cabria, H. B., Zamora, P. B., & Lapus, M. R. (2012). Terrestrial smokers: Thermal springs due to hydrothermal convection of groundwater connected to surface water. *Geophysical Research Letters*, *39*. https://doi.org/10.1029/2011gl050475

Carpenter, K. E., Abrar, M., Aeby, G., Aronson, R. B., Banks, S., Bruckner, A., et al. (2008). One-third of reef-building corals face elevated extinction risk from climate change and local impacts. *Science*, *321*(5888), 560–563. https://doi.org/10.1126/science.1159196

Carpenter, K. E., & Springer, V. G. (2005). The center of the center of marine shore fish biodiversity: The Philippine Islands. *Environmental Biology of Fishes*, *72*(4), 467–480. https://doi.org/10.1007/s10641-004-3154-4

Chiodini, G., Caliro, S., Cardellini, C., Avino, R., Granieri, D., & Schmidt, A. (2008). Carbon isotopic composition of soil CO2 efflux, a powerful method to discriminate different sources feeding soil CO_2 degassing in volcanic-hydrothermal areas. *Earth and Planetary Science Letters*, *274*(3-4), 372–379. https://doi.org/10.1016/j.epsl.2008.07.051

Christie, P. (2005). Observed and perceived environmental impacts of marine protected areas in two Southeast Asia sites. *Ocean & Coastal Management*, *48*(3-6), 252–270. https://doi.org/10.1016/j.ocecoaman.2005.04.012

Crook, E. D., Cohen, A. L., Rebolledo-Vieyra, M., Hernandez, L., & Paytan, A. (2013). Reduced calcification and lack of acclimatization by coral colonies growing in areas of persistent natural acidification. *Proceedings of the National Academy of Science of the United States of America*, *110*(27), 11,044–11,049. https://doi.org/10.1073/pnas.1301589110

del Rosario, R. A., & Oanes, A. F. (2010). *Controlled source magnetotelluric survey of Mabini Geothermal Prospect, Mabini, Batangas, Philippines, paper presented at World Geothermal Congress*. Bali, Indonesia: International Geothernal Association.

Erler, D. V., Shepherd, B. O., Linsley, B. K., Lough, J. M., & Cantin, N. E. (2018). Coral skeletons record increasing agriculture-related groundwater nitrogen inputs to a South Pacific Reef over the past century. *Geophysical Research Letters*, *45*(16), 8370–8378. https://doi.org/10.1029/2018gl078656

Fabricius, K. E., Langdon, C., Uthicke, S., Humphrey, C., Noonan, S., De'ath, G., et al. (2011). Losers and winners in coral reefs acclimatized to elevated carbon dioxide concentrations. *Nature Climate Change*, *1*(3), 165–169. https://doi.org/10.1038/nclimate1122

Forster, H., Oles, D., Knittel, U., Defant, M. J., & Torres, R. C. (1990). The Macolod Corridor-A rift crossing the Philippine Island-Arc. *Tectonophysics*, *183*(1-4), 265–271. https://doi.org/10.1016/0040-1951(90)90420-D

Funk, C. C., Peterson, P. J., Landsfeld, M. F., Pedreros, D. H., Verdin, J. P., Rowland, J. D., et al. (2014). *A quasi-global precipitation time series for drought monitoring, U.S. Geological Survey Data Series 832*. Reston VA: U. S. Geological Survey.

Gerlach, T. M., & Taylor, B. E. (1990). Carbon isotope constraints on degassing of carbon-dioxide from Kilauea Volcano. *Geochimica Et Cosmochimica Acta*, *54*(7), 2051–2058. https://doi.org/10.1016/0016-7037(90)90270-U

Goffredo, S., Prada, F., Caroselli, E., Capaccioni, B., Zaccanti, F., Pasquini, L., et al. (2014). Biomineralization control related to population density under ocean acidification. *Nature Climate Change*, *4*(7), 593–597. https://doi.org/10.1038/nclimate2241

Hall-Spencer, J. M., Rodolfo-Metalpa, R., Martin, S., Ransome, E., Fine, M., Turner, S. M., et al. (2008). Volcanic carbon dioxide vents show ecosystem effects of ocean acidification. *Nature*, *454*(7200), 96–99. https://doi.org/10.1038/nature07051

Hughes, T. P., Baird, A. H., Bellwood, D. R., Card, M., Connolly, S. R., Folke, C., et al. (2003). Climate change, human impacts, and the resilience of coral reefs. *Science*, *301*(5635), 929–933. https://doi.org/10.1126/science.1085046

Hughes, T. P., Barnes, M. L., Bellwood, D. R., Cinner, J. E., Cumming, G. S., Jackson, J. B. C., et al. (2017). Coral reefs in the Anthropocene. *Nature*, *546*(7656), 82–90. https://doi.org/10.1038/nature22901

Inoue, S., Kayanne, H., Yamamoto, S., & Kurihara, H. (2013). Spatial community shift from hard to soft corals in acidified water. *Nature Climate Change*, *3*(7), 683–687. https://doi.org/10.1038/nclimate1855

Kim, G., Kim, J. S., & Hwang, D. W. (2011). Submarine groundwater discharge from oceanic islands standing in oligotrophic oceans: Implications for global biological production and organic carbon fluxes. *Limnology and Oceanography*, *56*(2), 673–682. https://doi.org/10.4319/lo.2011.56.2.0673

Luz, B., & Barkan, E. (2010). Variations of O-17/O-16 and O-18/O-16 in meteoric waters. *Geochimica Et Cosmochimica Acta*, *74*(22), 6276–6286. https://doi.org/10.1016/j.gca.2010.08.016

Moore, W. S. (1996). Large groundwater inputs to coastal waters revealed by Ra-226 enrichments. *Nature*, *380*(6575), 612–614.

Munday, P. L., Cheal, A. J., Dixson, D. L., Rummer, J. L., & Fabricius, K. E. (2014). Behavioural impairment in reef fishes caused by ocean acidification at CO2 seeps. *Nature Climate Change*, *4*(6), 487–492. https://doi.org/10.1038/nclimate2195

Roberts, C. M., McClean, C., Veron, J. E., Hawkins, J. P., Allen, G. R., McAllister, D., et al. (2002). Marine biodiversity hotspots and conservation priorities for tropical reefs. *Science*, *295*(5558), 1280–1284. https://doi.org/10.1126/science.1067728

Samaniego, B. R., & Rebancos, C. M. (2019). The perceived benefits of marine protected areas by fishers in Batangas, Philippines. *Journal of Environmental Science and Management*, *22*(1), 1–12.

Santos, I. R., Eyre, B. D., & Huettel, M. (2012). The driving forces of porewater and groundwater flow in permeable coastal sediments: A review. *Estuarine, Coastal and Shelf Science*, *98*, 1–15.

Sawyer, A. H., David, C. H., & Famiglietti, J. S. (2016). Continental patterns of submarine groundwater discharge reveal coastal vulnerabilities. *Science*, *353*(6300), 705–707. https://doi.org/10.1126/science.aag1058

Sharp, Z. D. (2006). *Principles of Stable Isotope Geochemistry*. Upper Saddle River, New Jersey: Prentice Hall.

Spalding, M. D., & Brown, B. E. (2015). Warm-water coral reefs and climate change. *Science*, *350*(6262), 769–771. https://doi.org/10.1126/science.aad0349

Tait, D. R., Erler, D. V., Santos, I. R., Cyronak, T. J., Morgenstern, U., & Eyre, B. D. (2014). The influence of groundwater inputs and age on nutrient dynamics in a coral reef lagoon. *Marine Chemistry*, *166*, 36–47. https://doi.org/10.1016/j.marchem.2014.08.004

Tamayo, N. C. A., Anticamara, J. A., & Acosta-Michlik, L. (2018). Estimates of values of Philippine reefs' ecosystem services. *Ecological Economics*, *146*, 633–644. https://doi.org/10.1016/j.ecolecon.2017.12.005

Yardley, B. W. D. (2009). The role of water in the evolution of the continental crust. *Journal of the Geological Society*, *166*(4), 585–600. https://doi.org/10.1144/0016-76492008-101

Zamora, P. B., Cardenas, M. B., Lloren, R., & Siringan, F. P. (2017). Seawater-groundwater mixing in and fluxes from coastal sediment overlying discrete fresh seepage zones: A modeling study. *Journal of Geophysical Research-Oceans*, *122*(8), 6565–6582. https://doi.org/10.1002/2017jc012769

Zhou, Y. Q., Sawyer, A. H., David, C. H., & Famiglietti, J. S. (2019). Fresh submarine groundwater discharge to the near-global coast. *Geophysical Research Letters*, *46*(11), 5855–5863. https://doi.org/10.1029/2019gl082749